

RESEARCH ARTICLE



Development of a Novel Quantum Pre-processing Filter to Improve Image Classification Accuracy of Neural Network Models

Farina Riaz^{1,*}, Shahab Abdulla² , Hajime Suzuki¹, Srinjoy Ganguly², Ravinesh C. Deo³ and Susan Hopkins²

¹Data61, Commonwealth Scientific and Industrial Research Organisation, Australia

²UniSQ College, University of Southern Queensland, Australia

³School of Mathematics, Physics and Computing, University of Southern Queensland, Australia

Abstract: This paper proposes a novel quantum pre-processing filter (QPF) to improve the image classification accuracy of neural network (NN) models. A simple four qubit quantum circuit that uses Y rotation gates for encoding and two controlled NOT gates for creating correlation among the qubits is applied as a feature extraction filter prior to passing data into the fully connected NN architecture. By applying the QPF approach, the results show that the image classification accuracy based on the MNIST (handwritten 10 digits) and the EMNIST (handwritten 47 class digits and letters) datasets can be improved, from 92.5% to 95.4% and from 68.9% to 75.9%, respectively. These improvements were obtained without introducing extra model parameters or optimizations in the machine learning process. However, tests performed on the developed QPF approach against a relatively complex German Traffic Sign Recognition Benchmark dataset with 43 distinct class real-life traffic sign images showed a degradation in the classification accuracy. Considering this result, further research into the understanding and the design of a more suitable quantum circuit approach for image classification NNs could be explored utilizing the baseline method proposed in this paper.

Keywords: quantum machine learning, pre-processing filter, 2CNOT, quantum image classification

1. Introduction

The application of quantum computing to the tasks of machine learning, herein referred as quantum machine learning, has attracted much research attention in recent years. Literature surveys on quantum machine learning can be found in [1–4]. Among many proposals to combine classical machine learning methods with quantum computing, quanvolutional neural network (QNN) proposed by Henderson et al. [5] has an advantage of being implementable on quantum circuits with a smaller number of qubits with shallow gate depths and yet being applicable to practical applications. QNN utilizes quantum circuits as transformation layers, called quanvolutional layer, to extract features for the purpose of image classification using convolutional neural networks (CNNs). In Henderson et al. [5], MNIST handwritten 10-digit dataset [6] was applied to QNN using 9 qubits. The results showed classification accuracy improvement using QNN over CNN. However, when the quanvolutional layer of QNN was replaced by a conventional convolutional layer, no improvement in classification accuracy was observed. Henderson et al. later updated QNN and implemented on Rigetti Computing's Aspen-725Q-B quantum processing unit which has 25 qubits with 24 programmable

two-qubit gate interactions [7]. The proposed method was applied to 4 class low-resolution satellite image dataset. However, no improvement in classification accuracy by QNN over CNN was observed in Henderson et al. [7].

An implementation of QNN on a software quantum computing simulator, PennyLane [8], was provided by Mari [9]. Mari's implementation of QNN differs from that of Henderson in that the output of the quantum circuit, which is a set of expectation values, is directly fed into the following neural network (NN) layer, while that of Henderson was made into a single scalar value by a classical method. The proposed method was applied to MNIST dataset using 50 training and 30 test image sets. No clear improvement in classification accuracy by QNN over NN was observed in Mari [9]. A number of models utilizing QNN have been presented, including our own research that seeks to expand on Mari's work [10–17]. We used a strongly entangling quantum circuit in our investigation and showed improvements over Mari's observations [18].

Furthermore, the idea of quantum-enhanced convolutional networks has been expanded in recent studies. The quantum convolutional neural network (QCNN) for instance was proposed by Cong et al. and extends quantum convolutional layers with use of variational quantum parameters and how it can be used for error correction [19]. Yousif et al. conducted a further significant study on quantum CNN approaches, finding that integrating

*Corresponding author: Farina Riaz, Data61, Commonwealth Scientific and Industrial Research Organisation, Australia. Email: farina.riaz@csiro.au

quantum circuits with classical CNN improved performance in image classification tasks [20], proving enhancement in quantum-classical hybrid models training stability for COVID-19 datasets like and extends quantum convolutional layers to handle more complicated datasets, like covidx-cxr4 for feature extraction.

Despite these advancements, research into the possibilities of quantum-enhanced image classification is still ongoing. Prior studies have demonstrated only slight improvements in classification accuracy when comparing QNN to classical CNN (Henderson et al., Mari et al., etc.). This highlights a key field of research in effectively employing quantum methods to outperform classical ones. Furthermore, while hybrid quantum-classical approaches show promise, their full potential for real-life applications is still unexplored.

To address this gap, we introduce a novel approach, the quantum pre-processing filter (QPF), inspired by the QNNs proposed by Henderson and Mari. The QPF demonstrates significant improvements in image classification accuracy compared to counterpart CNNs. This work is designed as a foundational step toward exploring models that can be effectively applied in smart transportation systems, offering a robust framework for enhancing image-based decision-making in this domain. QPF uses a quantum circuit with four qubits, four Y rotations, two controlled NOTs (CNOTs), and four measurements.

degradation in classification accuracy by the application of QPF. This prompts further research into the understanding and design of suitable quantum circuits for image classification NNs. To support the validation of our claims and further research, we have made our source code available at <https://github.com/hajimesuzuki999/qpf>.

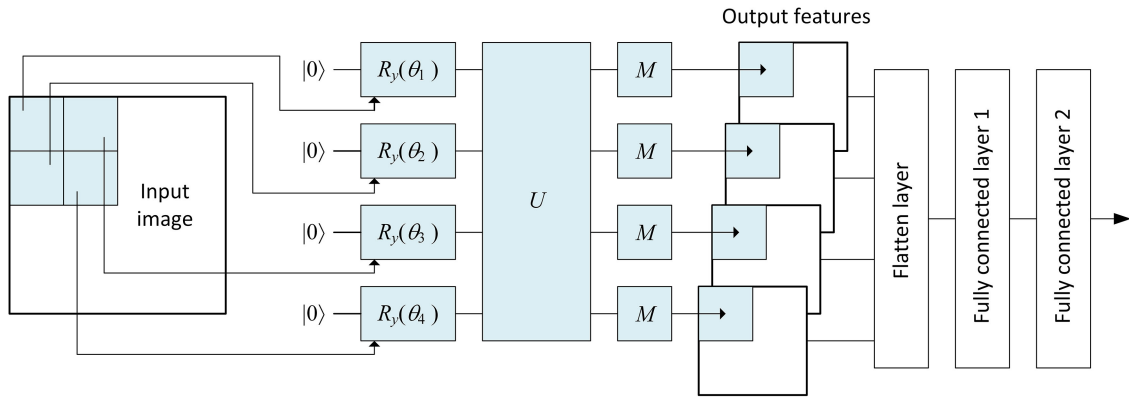
To further evaluate the model, we extended the analysis in our other paper [23]. We applied QPF model to binary classification tasks, validating it with two CNOT gates. Accuracy improved on MNIST, EMNIST, and CIFAR-10, while GTSRB showed an increase without QPF but a slight decrease when QPF was applied. Smaller datasets also benefited from QPF, showing modest accuracy gains.

This paper is organized as follows: The new QPF unit combined with the classical image classification NN is proposed in Section 2. Section 3 describes the experiment conducted using software simulation. The results and discussions are presented in Section 4, followed by conclusions in Section 5.

2. Methodology

Figure 1 shows the architecture of the proposed QPF model also explained in our extension paper of this work [23]. The method assumes that the input image is a two-dimensional matrix with size m -by- m and the pixel value, x , follows $0 \leq x \leq 1$. An

Figure 1
The architecture of the proposed quantum pre-processing filter (QPF) model



When QPF is applied as a pre-processing unit of an image classification NN, i.e., as a feature extraction filter, the image classification accuracy of fully connected NN against MNIST and EMNIST (handwritten 47 class digits and letters, Cohen et al. [21] improves from 92.5% to 95.4% and from 68.9% to 75.9%, respectively. These improvements were obtained without introducing any extra parameters to optimize in machine learning process. Unlike other quantum machine learning methods, the use of QPF does not require optimization of the parameters inside the quantum circuits and hence requires only a limited use of the quantum circuit. Given the small number of qubits and relatively shallow depth of the quantum circuit, QPF is well suited to be implemented on noisy intermediate-scale quantum computers. While the proposed method is promising, a test against a more complicated dataset, German Traffic Sign Recognition Benchmark (GTSRB) (43 class real-life traffic sign images [22]), showed

extension to multi-channel pixel image is considered as straightforward. Similar to QNN models, a section of size n -by- n is extracted from the input image. While $1 < n \leq m$ in the case of QNN, the proposed QPF uses $n=2$. This 2×2 section of the input image is referred as QPF window. An extension of QPF using $n > 2$ is left for further studies.

The methodology of this work is as follows. The input image is represented as a two-dimensional m -by- m matrix, where each pixel value x ranges between 0 and 1. Extending this approach to multi-channel images is straightforward. Each pixel value is then encoded into a quantum state using the R_Y gate, which rotates the Bloch sphere around the Y -axis by an angle $\theta = 2\pi x$, proportional to the pixel intensity x . This transformation converts classical pixel values into quantum states, enabling quantum processing of image data. Mathematically R_Y gate can be written as in Equation (1):

$$R_y(\theta) = \begin{bmatrix} \cos \frac{\theta}{2} & -i \sin \frac{\theta}{2} \\ \sin \frac{\theta}{2} & \cos \frac{\theta}{2} \end{bmatrix} \quad (1)$$

The QPF model processes the input image by extracting a small n -by- n portion, where n is the window size. In this approach, a 2×2 section of the image, called the QPF window, is selected. Each pixel within the window is encoded using the RY gate, which rotates qubits by an angle $\theta = 2\pi x$ based on pixel intensity. The encoded data are then processed through the quantum circuit of the QPF model, enabling localized feature extraction while controlling circuit complexity. The outputs from the RY gates are fed to a quantum circuit, denoted as U in Figure 1. This paper examines three different quantum circuits: the first, “Encoding Only” shown in Figure 2, performs measurement immediately after encoding; the second, “One CNOT” as in Figure 3, applies a controlled NOT operation with the first qubit as the control and the fourth qubit as the target; and the third, “Two CNOTs” as in Figure 4,

Figure 2
Quantum pre-processing filter, with encoding only

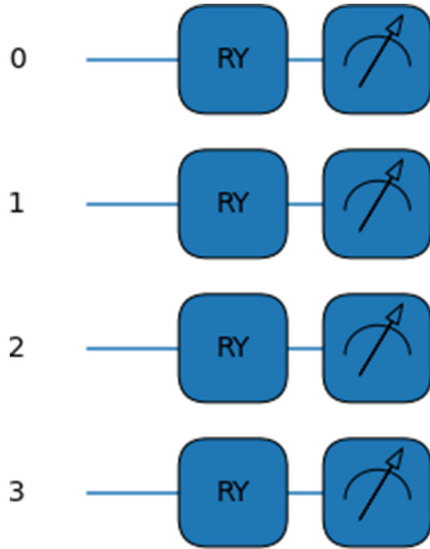


Figure 3
Quantum pre-processing filter, with one CNOT

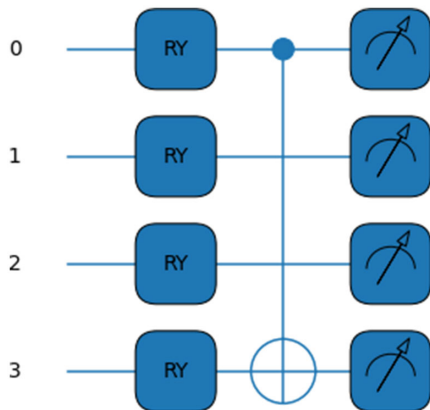
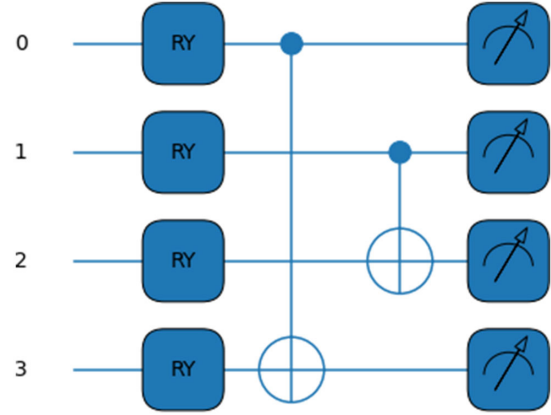


Figure 4
Quantum pre-processing filter, with two CNOTs



performs two controlled NOT operations for additional quantum processing.

Measurement operations, labeled as M in Figure 1, are conducted on the output from the quantum circuit U . These measurements produce expectation values ranging from -1 to 1 , which are then used as output features. It's important to highlight that the total number of parameters in the input image ($m \times m$) is the same as in the output features ($4 \times (m/2) \times (m/2)$). The output features are subsequently flattened into a one-dimensional vector, with the flattening layer containing $m \times m$ nodes. These nodes are fully connected in the first fully connected layer, while the second fully connected layer produces an output with a number of nodes equal to the number of classes. The experimental approach involved conducting multiple tests, with each combination being evaluated across 100 random iterations to ensure consistency and validity. By selecting distinct training and testing samples, statistically stable results were obtained, enhancing the robustness, minimizing biases, and improving the generalization of the findings for broader applications.

3. Experiment

As was performed by many, we first apply the proposed method to the MNIST dataset [6] to obtain benchmark results. The MNIST dataset consists of 60,000 training and 10,000 test images of handwritten digits of 0 to 9. The size of each image is 28 by 28 pixels. The original images are in grayscale within the values between 0 and 255, which are scaled by dividing them by 255. We then chose the EMNIST dataset [21] to extend the number of image class. The EMNIST dataset (Balanced and By Merge [21]) contains 112,800 training and 18,800 test images of handwritten digits and letters making up 47 classes. Note that some of upper- and lower-case letters are merged due to their similarity (e.g., C is similar to c) in this dataset. Original EMNIST dataset is divided by 255 to create a dataset with pixel values between 0 and 1.

The GTSRB dataset [22] consists of 34,799 training and 12,630 test images of 43 class traffic signs captured from actual traffic signs in use in various conditions. The original dataset has various image sizes between 15×15 and 222×193 pixels. Those images were scaled to a size of 32×32 pixels. The original images were in RGB color, which were converted into grayscale between 0 and 255. Unlike MNIST and EMNIST dataset, in order to normalize the dynamic range of each image, the normalization is applied to each image according to the following formula:

$$\tilde{c}_{x,y} = \frac{c_{x,y} - \min(I)}{\max(I) - \min(I)} \quad (2)$$

where $c_{x,y}$ and $\tilde{c}_{x,y}$ represent the original and normalized pixel values in the position (x,y) , and $\max(I)$ and $\min(I)$ denote the maximum and the minimum element in the two-dimensional image matrix I , respectively.

In order to make use of the advantages of each platform, the experiment was run on both MATLAB and PennyLane. Using PennyLane's ease of use in building and manipulating quantum operations, the quantum circuits were developed and simulated. After that, these quantum circuits were exported as unitary matrices to MATLAB, which can handle the quantum operations in a classical format. This made it possible for MATLAB to include the quantum features into its larger computing structure.

The Adam optimizer [24], which is well-known for its effectiveness in gradient-based optimization, has been applied to the QPF model. For all three datasets, a mini-batch size of 128 was used to guarantee robust evaluation of the model's performance across various data distributions. Both systems worked effectively when combined to evaluate the hybrid quantum-classical model, providing flexibility for both classical training methods and quantum circuit design.

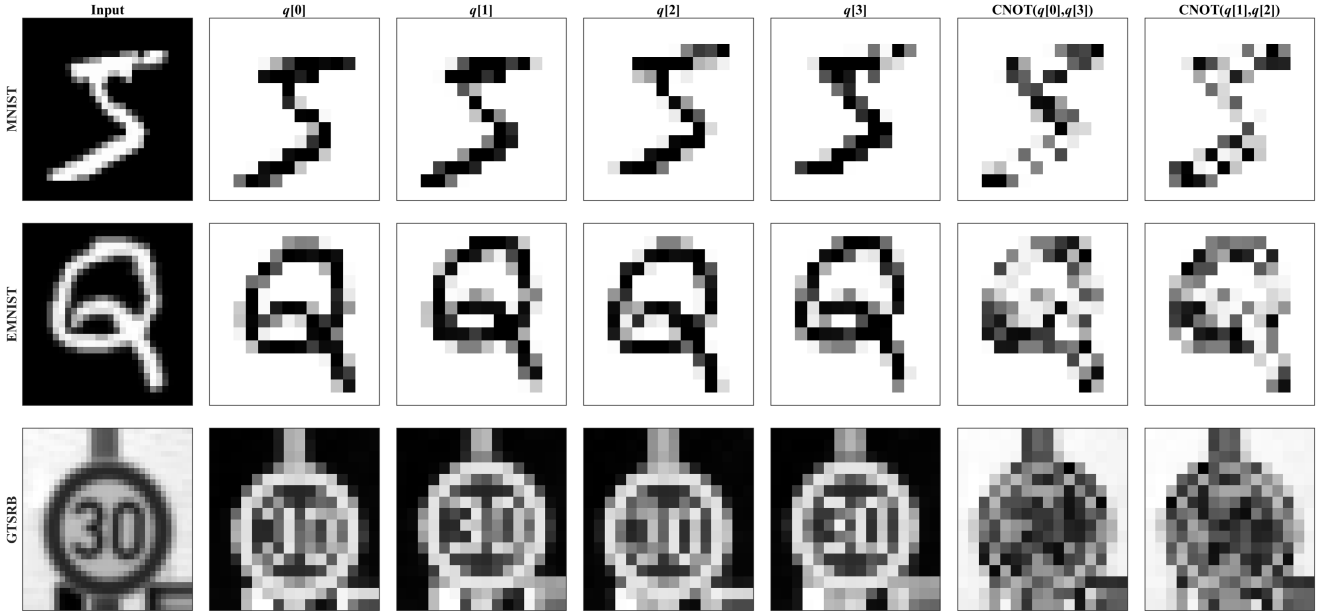
Three datasets MNIST, EMNIST, and GTSRB—as well as the corresponding outcome features generated during the quantum encoding process—are presented in Figure 5. Every input image is converted into one of three quantum states, represented by

subsequently utilized in later layers of the model to do further processing.

4. Result and Discussion

Using the MNIST dataset, Figure 6 shows how different QPF configurations affect the testing dataset accuracy as an outcome of training iterations. The graph illustrates how various quantum circuit designs impact the model's overall accuracy as well as its rate of convergence. The phenomenon of faster convergence was also observed in Henderson's QNN [5]. In comparison to a classical NN which involves directly passing raw pixel values to the NN. Our current classical NN already employs quantum filter approach; however, instead of applying a 4×4 pre-processing window in a loop, we process the entire image and pass it into fully connected layers, the QPF encoding-only model converges faster during training. This can be observed in Figure 6, where measurements are performed directly after encoding without any additional quantum operations. The faster convergence is comparable to what Henderson's QNN model demonstrated. Though the QPF encoding-only model converges more quickly, it still falls short of the traditional NN in terms of final test set accuracy. This implies that the full potential of quantum computation for increasing precision may not be realized by only encoding classical data into quantum states without introducing quantum entanglement.

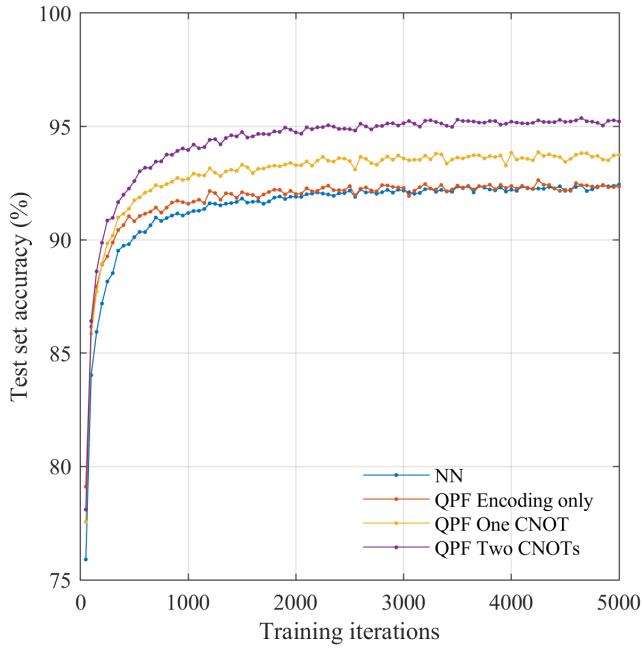
Figure 5
An example of the input image and the relevant output features



qubits and labeled $q[0]$ through $q[3]$. The results of quantum encoding alone can be seen in the image, along with the effects of using two controlled NOT (CNOT) operations: $\text{CNOT}(q[0], q[3])$ and $\text{CNOT}(q[1], q[2])$. These CNOT gates create quantum correlations between $q[0]$ and $q[3]$ and between $q[1]$ and $q[2]$ by entanglement of pairs of qubits. The input images' modified quantum states are captured by the output features that are shown following entanglement and encoding, and these features are

As demonstrated by the QPF One CNOT model, performance increases with the addition of a CNOT gate. Here, the final test set accuracy is improved from 92.5% (in the classical NN example) to 93.7% by applying a single CNOT operation across the first and fourth qubits after encoding. This implies that adding quantum entanglement between qubits improves the accuracy of the model by enabling it to extract more meaningful features from the data. When two CNOT gates are used in the QPF Two CNOTs model,

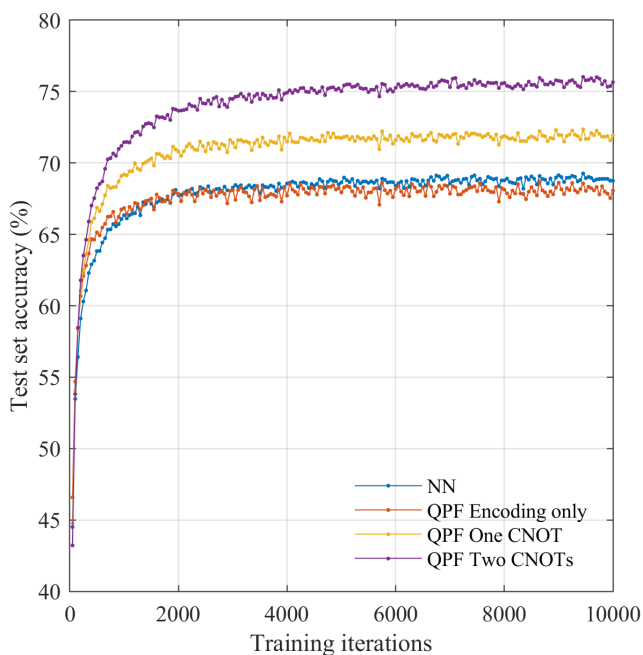
Figure 6
Test set accuracy using MNIST dataset



the accuracy is substantially improved. The accuracy of the test set increases to 95.4% by executing two entangling operations: one between the second and third qubits and one between the first and fourth qubits. This indicates that increasing the complexity of the quantum circuit, through greater entanglement, allows the model to better capture the underlying structure of the data, leading to higher accuracy in image categorization.

Using the EMNIST dataset, Figure 7 shows how various QPF settings affect the speed of convergence and accuracy of the final test

Figure 7
Test set accuracy using EMNIST dataset

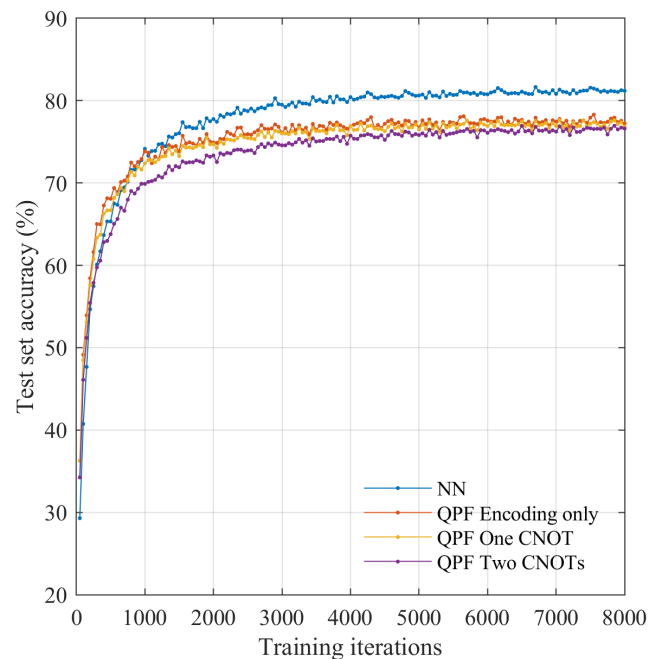


set. Comparing the use of QPF encoding only to the classical NN, the findings are like the MNIST results in terms of faster convergence. This indicates that the QPF encoding-only model reaches its performance plateau during training more quickly than the NN. This faster convergence implies that early in training, quantum encoding—even in the absence of entanglement—converts classical data into quantum states, speeding up the learning process. Though QPF encoding only achieves a faster convergence, the trained model's final accuracy is less than that of the classical NN. This indicates that the encoding-only quantum model lacks the complexity necessary to outperform the classical NN in terms of classification accuracy on the EMNIST dataset, even though it learns more quickly. The shortcomings of encoding-only quantum models, which do not incorporate the advantages of quantum entanglement and may aid the model in capturing greater complexity of connections in the data, may be the cause of this decrease in accuracy. The introduction of quantum entanglement through CNOT gates improves the circumstances. Like in the MNIST tests, a single CNOT gate is applied between the first and fourth qubits in the QPF One CNOT arrangement. From 68.9% (achieved by the classical NN) to 72.0% (achieved by the quantum circuit), the ultimate test set accuracy is improved by this extra layer of complexity. This finding implies that quantum entanglement improves the model's performance by boosting its capacity to extract meaningful features from the data.

The QPF Two CNOTs model, which entangles the qubits using two CNOT gates, gives the best accuracy. The test set accuracy is further increased to 75.9% by this more intricate quantum circuit, which is a considerable improvement over the simpler QPF configurations and the classical NN. The increase from 68.9% to 75.9% shows the effectiveness of using many CNOTs, or quantum operations, to extract more complex characteristics from the data. This is especially useful for datasets like EMNIST, which have more difficult image classification tasks.

Figure 8 shows the variation of test set accuracy using the GTSRB dataset. Unlike the cases using MNIST and EMNIST

Figure 8
Test set accuracy using GTSRB dataset



datasets, the converged test set accuracy by the application of QPF is reduced from that of NN in the case of GTSRB dataset. The exact causes of this phenomenon are currently unknown to the authors and remain for further research. The summary of the testing accuracy results is shown in Table 1.

Table 1
Summary of testing accuracy results

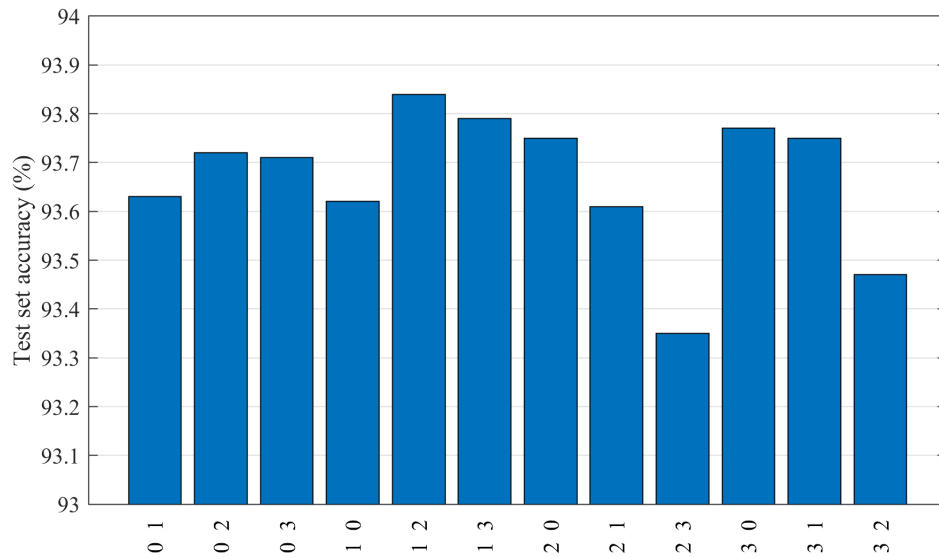
	MNIST	EMNIST	GTSRB
NN	92.5%	68.9%	81.4%
Encoding only	92.4%	68.1%	77.6%
One CNOT	93.7%	72.0%	77.6%
Two CNOT	95.4%	75.9%	77.0%

Referring back to Figure 3, there are 12 different ways to create a CNOT circuit from four qubits. In order to investigate if a different CNOT arrangement would make the difference in classification accuracy, the training of the network and the classification of the images were performed for MNIST dataset using the 12 different CNOT arrangements. Figure 9 shows the results. The x axis of Figure 9 denotes the arrangement of the CNOT where the lower number refers to the control qubit and the upper number refers to the target qubit.

of the second CNOT. For example, “0 3 1 2” refers to the arrangement as shown in Figure 4. As evident in Figure 10, the CNOT arrangements pairing the 1st and the 4th qubits and pairing the 2nd and the 3rd qubits seem to achieve a higher testing accuracy irrespective of which qubit is assigned as the target or the control. Referring back to Figure 1, the pairing of the 1st and 4th qubits and the pairing of the 2nd and 3rd qubits correspond to the pairing of the diagonal elements of the 2×2 QPF window. The exact reason for the improved classification accuracy in the case of MNIST and EMNIST datasets when correlating the diagonal elements of the QPF window is currently not known to the authors and is left for further research.

The results presented in this study highlight some promising improvements in feature extraction for simpler datasets like MNIST and EMNIST using the QPF. Establishing a classical pre-processing baseline involves directly passing raw pixel values to the NN. Our current classical NN already employs this classical counterpart of pre-processing; however, instead of applying a 4×4 pre-processing window in a loop, we process the entire image and pass it into fully connected layers to reduce computational overhead. No additional pre-processing steps are applied before passing the data to the fully connected layers. Classical systems don’t exhibit quantum phenomena like superposition and entanglement, which are essential for quantum algorithms. Using a quantum simulator, we model these effects, including the wave-like behavior of superposition, where

Figure 9
Test set accuracy on MNIST dataset using different CNOT arrangements

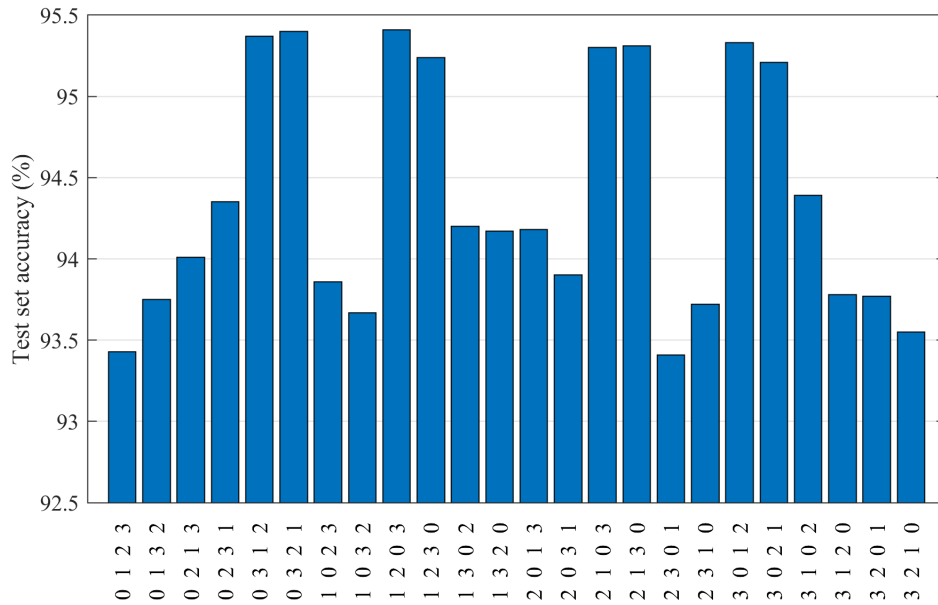


For example, “0 3” refers to the arrangement as shown in Figure 3. As can be seen from Figure 9, the variation of test set accuracy for different CNOT arrangement is considered to be small, within less than 0.6%.

Similarly, there are 24 different ways to arrange the two CNOTs using four qubits. The test set accuracy was derived for 24 different two CNOTs arrangement using MNIST dataset, and the results are shown in Figure 10. In Figure 10, the x axis label refers to the arrangement of the two CNOTs in the order of the control and target qubits of the first CNOT, then the control and target qubits

quantum states exist in multiple possibilities with associated probabilities. This allows us to study how these quantum behaviors, including interference, impact the performance of quantum algorithms, even without real quantum hardware. Superposition and entanglement can be generated using quantum gates such as RY and CNOT. Classical machine learning already excels with optimized tools, and these classical systems can approximate some quantum behaviors with increased computational effort, they generally cannot fully capture the complexity or scale of quantum effects.

Figure 10
Test set accuracy on MNIST dataset using different two CNOTs arrangements



Additionally, the current configuration of the QPF, utilizing only four qubits, may be insufficient for capturing the complex feature hierarchies required for more intricate datasets like the GTSRB. The lack of improvement on more complex datasets suggests that the quantum pre-processing method may not be able to extract the necessary features for such datasets in its current form. Increasing the number of qubits in the QPF could potentially improve its ability to encode more complex features and enhance performance on more challenging datasets.

To understand the performance improvement, the QPF's entanglement arrangement has a significant impact on how well it extracts features. By creating correlations between qubits, entanglement allows the quantum system to encode complex relationships in the input data. Nonetheless, the QPF's performance across datasets indicates that, depending on the complexity of the dataset, the current entanglement technique may have varying effects on its capacity to capture features. The two CNOT entanglement arrangement works well for capturing basic relationships in the data, like the forms and structures of characters and numbers, for datasets that are simpler, like MNIST and EMNIST. The present entanglement structure effectively encodes the relatively simple feature hierarchies needed by these datasets, improving classification performance.

In contrast, for more complex datasets such as GTSRB, which include images with diverse conditions (e.g., varying lighting, angles, and noise), the current entanglement scheme shows limitations. The 2-CNOT configuration lacks the flexibility or capacity to encode the intricate and high-dimensional feature spaces required for the accurate classification of these challenging datasets. This suggests that the current entanglement structure may not fully exploit the potential of quantum systems for complex data representations.

To improve the QPF's performance on such datasets, adjustments to the entanglement design are necessary. These may include increasing the number of qubits, introducing additional entanglement layers, or exploring more advanced entanglement strategies. Furthermore, integrating the QPF with classical models,

such as CNNs, could provide a complementary approach to capture multi-scale feature hierarchies. This analysis highlights the importance of optimizing the entanglement configuration to better leverage quantum phenomena for feature extraction, particularly for datasets with greater complexity.

5. Conclusion

In this study, a novel QPF was introduced to enhance image classification accuracy in NNs, particularly for simpler datasets like MNIST and EMNIST. By leveraging quantum operations, the QPF modifies input data before passing it to the NN, improving the pre-processing stage of the classification pipeline. Our experiments demonstrated significant improvements in classification performance for datasets with simple images (lower-dimensional data), such as handwritten digits and characters, attributed to quantum characteristics like superposition and entanglement enabling better feature extraction. However, for more complex datasets (higher-dimensional data), such as the GTSRB, the QPF did not achieve comparable improvements. These complex datasets involve richer, multi-dimensional feature spaces and intricate relationships that require deeper feature hierarchies, which the current QPF configuration struggles to capture effectively. This highlights the need for further optimization of the QPF configuration to better capture the intricate feature hierarchies required by these datasets. Future research should explore increasing the number of qubits to enhance the QPF's capacity for encoding complex, high-dimensional data and consider integrating it with advanced models like CNNs. The combination of quantum pre-processing with classical machine learning holds significant potential for advancing image classification. While the current findings highlight the promise of the QPF for simpler datasets, further refinement and experimentation are necessary to expand its applicability to more challenging datasets, paving the way for broader adoption of quantum techniques in machine learning.

Acknowledgement

This research has been supported by Australian Government Research Training Program and Commonwealth Scientific Industrial and Research Organization.

Ethical Statement

This study does not contain any studies with human or animal subjects performed by any of the authors.

Conflicts of Interest

The authors declare that they have no conflicts of interest to this work.

Data Availability Statement

The data that support the findings of this study are openly available in GitHub at <https://github.com/hajimesuzuki999/qpf>.

Author Contribution Statement

Farina Riaz: Conceptualization, Methodology, Software, Validation, Formal analysis, Investigation, Resources, Data curation, Writing – original draft, Writing – review & editing, Visualization, Project administration. **Shahab Abdulla:** Validation, Formal analysis, Investigation, Resources, Data curation, Writing – original draft, Writing – review & editing, Supervision. **Hajime Suzuki:** Methodology, Validation, Formal analysis, Investigation, Resources, Data curation, Writing – original draft, Writing – review & editing, Visualization, Supervision, Project administration. **Srinjoy Ganguly:** Conceptualization, Methodology, Software, Validation, Formal analysis, Investigation, Resources, Data curation, Writing – original draft, Writing – review & editing, Visualization, Supervision, Project administration. **Ravinesh C. Deo:** Investigation, Resources, Data curation, Writing – review & editing, Supervision. **Susan Hopkins:** Writing – review & editing, Supervision.

References

- [1] Benedetti, M., Lloyd, E., Sack, S., & Fiorentini, M. (2019). Parameterized quantum circuits as machine learning models. *Quantum Science and Technology*, 4(4), 043001.
- [2] Peral-García, D., Cruz-Benito, J., & García-Peñalvo, F. J. (2024). Systematic literature review: Quantum machine learning and its applications. *Computer Science Review*, 51, 100619.
- [3] O'Quinn, W., & Mao, S. (2020). Quantum machine learning: Recent advances and outlook. *IEEE Wireless Communications*, 27(3), 126–131.
- [4] Gong, L. H., Pei, J. J., Zhang, T. F., & Zhou, N. R. (2024). Quantum convolutional neural network based on variational quantum circuits. *Optics Communications*, 550, 129993.
- [5] Henderson, M., Shakyia, S., Pradhan, S., & Cook, T. (2020). Quadvolutional neural networks: Powering image recognition with quantum circuits. *Quantum Machine Intelligence*, 2(1), 2.
- [6] LeCun, Y., Bottou, L., Bengio, Y., & Haffner, P. (1998). Gradient-based learning applied to document recognition. *Proceedings of the IEEE*, 86(11), 2278–2324.
- [7] Henderson, M., Gallina, J., & Brett, M. (2021). Methods for accelerating geospatial data processing using quantum computers. *Quantum Machine Intelligence*, 3(1), 4.
- [8] Bergholm, V., Izaac, J., Schuld, M., Gogolin, C., Ahmed, S., Ajith, V., . . . , & Killoran, N. (2018). PennyLane: Automatic differentiation of hybrid quantum-classical computations. *arXiv Preprint:1811.04968*.
- [9] Mari, A. (2021). *Quadvolutional neural network*. Retrieved from: <https://pennylane.ai/qml/demos/tutorialquadvolution.html>
- [10] Li, Y., Liu, R., Hao, X., Shang, R., Zhao, P., & Jiao, L. (2023). EQNAS: Evolutionary quantum neural architecture search for image classification. *Neural Networks*, 168, 471–483.
- [11] Abdel-Khalek, S., Algarni, M., Mansour, R. F., Gupta, D., & Ilayaraja, M. (2023). Quantum neural network-based multilabel image classification in high-resolution unmanned aerial vehicle imagery. *Soft Computing*, 27(18), 1–12.
- [12] Chen, G., Chen, Q., Long, S., Zhu, W., Yuan, Z., & Wu, Y. (2023). Quantum convolutional neural network for image classification. *Pattern Analysis and Applications*, 26(2), 655–667.
- [13] Bai, Q., & Hu, X. (2023). Quantity study on a novel quantum neural network with alternately controlled gates for binary image classification. *Quantum Information Processing*, 22(5), 184.
- [14] Wang, A., Hu, J., Zhang, S., & Li, L. (2024). Shallow hybrid quantum-classical convolutional neural network model for image classification. *Quantum Information Processing*, 23(1), 17.
- [15] Wu, S., Li, R., Song, Y., Qin, S., Wen, Q., & Gao, F. (2024). Quantum assisted hierarchical fuzzy neural network for image classification. *IEEE Transactions on Fuzzy Systems*, 33(1), 491–502.
- [16] Shi, M., Situ, H., & Zhang, C. (2024). Hybrid quantum neural network structures for image multi-classification. *Physica Scripta*, 99(5), 056012.
- [17] Senokosov, A., Sedykh, A., Sagingalieva, A., Kyriacou, B., & Melnikov, A. (2024). Quantum machine learning for image classification. *Machine Learning: Science and Technology*, 5(1), 015040.
- [18] Riaz, F., Abdulla, S., Suzuki, H., Ganguly, S., Deo, R. C., & Hopkins, S. (2023). Accurate image multi-class classification neural network model with quantum entanglement approach. *Sensors*, 23(5), 2753.
- [19] Cong, I., Choi, S., & Lukin, M. D. (2019). Quantum convolutional neural networks. *Nature Physics*, 15(12), 1273–1278.
- [20] Yousif, M., & Al-Khateeb, B. (2024). Quantum convolutional neural network for image classification. *Fusion: Practice & Applications*, 15(2), 61–72.
- [21] Cohen, G., Afshar, S., Tapson, J., & Van Schaik, A. (2017). EMNIST: Extending MNIST to handwritten letters. In *2017 International Joint Conference on Neural Networks*, 2921–2926.
- [22] Stallkamp, J., Schlipsing, M., Salmen, J., & Igel, C. (2011). The German traffic sign recognition benchmark: A multi-class classification competition. In *The 2011 International Joint Conference on Neural Networks*, 1453–1460.
- [23] Riaz, F., Abdulla, S., Suzuki, H., Ganguly, S., Deo, R. C., & Hopkins, S. (2024). The application of quantum pre-processing filter for binary image classification with small samples. *Journal of Data Science and Intelligent Systems*, 3(2), 79–164. <https://doi.org/10.47852/bonviewJDSIS42024229>
- [24] Kingma, D. P. (2014). Adam: A method for stochastic optimization. *arXiv Preprint:1412.6980*.

How to Cite: Riaz, F., Abdulla, S., Suzuki, H., Ganguly, S., Deo, R. C., & Hopkins, S. (2025). Development of a Novel Quantum Pre-processing Filter to Improve Image Classification Accuracy of Neural Network Models. *Journal of Data Science and Intelligent Systems*. <https://doi.org/10.47852/bonviewJDSIS52024231>